The reversible phase transition of DNA-linked colloidal gold assemblies

Young Sun, Nolan C. Harris, Ching-Hwa Kiang*

Department of Physics and Astronomy, Rice University, Houston, TX 77005-1892, USA

Abstract

We present direct evidence for a reversible phase transition of DNA-linked colloidal gold assemblies. Transmission electron microscopy and optical absorption spectroscopy are used to monitor the colloidal gold phase transition, whose behavior is dominated by DNA interactions. We use single-stranded DNA-capped colloidal gold that is linked by complementary linker DNA to form the assemblies. We found that, compared to free DNA, a sharp melting transition is observed for the DNA-linked colloidal gold assemblies. The structure of the assemblies is non-crystalline, much like a gel phase, consistent with theoretical predictions. Optical spectra and melting curves provide additional evidence of gelation of the colloidal system. The phase transition and separation are examples of percolation in a dilute solvent.
© 2005 Elsevier B.V. All rights reserved.

*Corresponding author. Tel.: +1 713 348 4130; fax: +1 713 348 4150.
E-mail address: chkiang@rice.edu (C.-H. Kiang).

1. Introduction

Colloidal nanoparticles functionalized and linked with single-stranded DNA exemplify a new class of complex fluids. Both equilibrium and nonequilibrium phase transitions of complex particle systems are of great interest [1,2]. The interaction between colloidal particles is controlled by the DNA intermolecular potentials, which are dominated by hydrogen bonding. Owing to the complex yet specific nature of DNA base pairing, the interaction between colloids in such a system can be precisely controlled and ''tailor made'' to have a specific potential. Both the number of components and the strength of the interaction forces can be designed. A variety of different states of this system have been investigated theoretically [3,4].

DNA melting and hybridization, an important process in DNA replication and translation, have been studied for decades [5–12]. Many of the thermodynamic properties of free DNA are known, yet DNA interactions in constrained spaces such as on surfaces, e.g. in microarrays, are still poorly understood [13]. The sequence-specific hybridization properties of DNA have been used for self-assembly of nanostructures [14,15]. The macroscopic properties of these novel systems can be easily detected and are a result of the microscopic properties of DNA. Thus, studies of the phase behavior of these self-assemblies provide valuable information on fundamental DNA properties [3,16,17].

DNA-linked gold colloids were thought to self-assemble into crystalline structures [14]; however, it was proposed by Kiang [18] that the structure of the assemblies is amorphous, much like a percolating cluster. Calculated optical spectra are consistent with an amorphous structure [16]. The phase behavior of this system has also been investigated theoretically, and it is believed that the system undergoes a liquid–liquid phase separation, with the dense liquid phase behaving as a solid (amorphous) gel [3]. More experimental studies of the structural phase transition are needed to unravel the true nature of the phase transition, which is crucial in understanding the behavior of such multi-component complex fluids.

Direct imaging is a powerful tool to study the structures arising during the colloidal phase transition [19], and the results can be interpreted unambiguously. In this paper, we present evidence of a liquid–gel phase transition of DNA-linked gold colloid assemblies via direct imaging. The aggregation and phase transition of the DNA-linked gold colloids were studied using transmission electron microscopy (TEM) [20] and optical absorption spectroscopy. The results obtained suggest that gelation and phase separation occurs at room temperature in the DNA-linked gold colloid system.

2. Results and discussion

To prepare colloidal systems with different interactions, we start with a range of sizes of gold nanoparticles (10–40 nm, < 10% polydispersity) capped with either $3'$ or $5'$ modified, single-stranded, 12-base DNA. The basic building block is illustrated in Fig. 1. Details of the sample preparation are described in Ref. [18]. We added linker
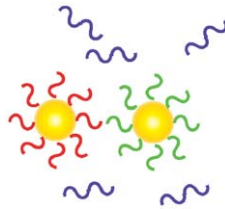
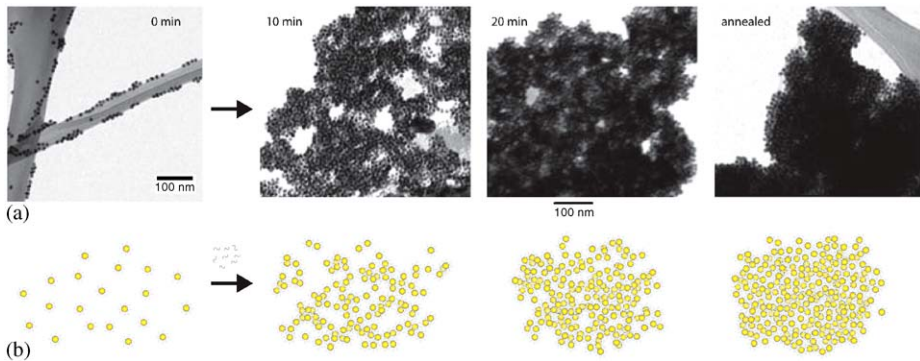Fig. 1. The basic building block of DNA-linked gold particles.

Fig. 2. (a) Sequence of transmission electron microscopy images of 10 nm gold colloids capped with thiol-modified DNA. The colloids are initially dispersed in solution, upon adding linker DNA, gold colloids form gel-like porous and amorphous aggregates. Phase separation occurs, and eventually the dense aggregates precipitate out of the solution. (b) The growth mechanism of DNA-linked gold colloids. The colloids are initially dispersed in solution. Upon adding linker DNA, gold colloids form gel-like porous and amorphous aggregates. Phase separation occurs, and eventually the dense aggregates precipitate out of the solution.

DNA, which caused the nanoparticles to form aggregates, and we studied the melting transition with microscopy and spectroscopy.

We propose the growth mechanism of DNA-linked gold colloids (illustrated in Fig. 2b) to be as follows. Particles initially are dissolved in the solution. With the addition of complementary linker DNA, hybridization occurs, and the particles form a gel-like structure. The connectivity of the porous structure continues to increase past the percolation threshold, and eventually the clusters become a dense amorphous structure. Phase separation occurs and the gel-like aggregates eventually precipitate out of the solution.

Direct imaging using TEM supports this model. Fig. 2a displays a series of TEM images taken at different aggregation stages. Before adding linker DNA, the DNA-capped gold particles are dispersed in the solution. Upon adding linker DNA, the colloidal gold forms aggregates. The process is reversed by raising the temperature above the transition temperature.

UV-visible absorption spectroscopy is a powerful tool to study the aggregation and phase transition of the DNA-linked gold colloids because DNA bases and gold colloids have strong absorption in the UV region ($\sim$260 nm) and the visible light region ($\sim$520 nm), respectively. The extinction coefficient as well as the peak position are sensitive to the size of the aggregates of gold colloids. The DNA double helix has a smaller extinction coefficient than does single-stranded DNA due to hypocromism [21]. Thus, both the kinetics of colloidal aggregation and the temperature-dependent melting transition can be investigated using UV-visible spectroscopy. All spectra were taken on a PerkinElmer Lambda 45 spectrophotometer.

Upon adding linker DNA, gold nanoparticles begin to aggregate, as indicated by the change of the UV absorption. The aggregation rate at room temperature is faster for systems with higher T_m. Solutions of DNA-linked gold colloids were allowed to stand at room temperature for several days for the system to fully aggregate before melting studies. We monitor the absorption intensity at 260 and 520 nm while slowly heating the DNA-linked gold colloids. The sample was heated by a peltier temperature controller from 25 to 75 °C at a rate of 0.5 °C/min. The 260 and 520 nm melting curves are very similar, indicating that DNA and gold colloid melting are closely related. Fig. 3 shows the melting curves of 10, 20, and 40 nm gold colloids with linker DNA. For comparison, the melting transition of a free DNA is also shown. Apparently, the melting transition of gold-attached DNA is much narrower than that of free DNA.

The melting temperature T_m, defined as the temperature at the midpoint of the absorbency transition [22], is found to be a function of particle diameter, D, and the data are fitted to $T_m(°C) = 68 - 57/\sqrt{D}$. The surface coverage of thiol-capped DNA bound to gold nanoparticles has been determined via the fluorescence method to be approximately 160 DNA (12-mer) bound for a 16 nm diameter particle [23]. Assuming that the number of DNA bound to gold particles scales with the particle surface area, D^2, there are 50, 190, and 750 DNA on 10, 20, and 40 nm particles, respectively. An increasing number of connections between particles as the gold particle size increases is expected. Since the hydrogen bonding energy per DNA pair
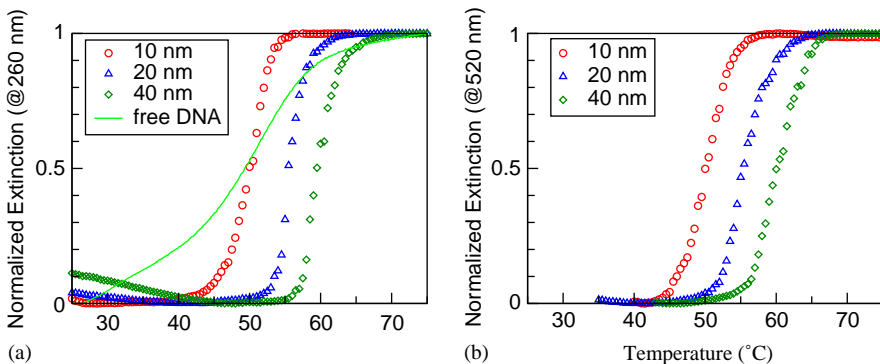

Fig. 3. Melting curves for *AB* nanoparticle systems monitored at (a) 260 nm and (b) 520 nm. The free DNA melting curve monitored at 260 nm is shown in (a).

remain the same, an increased number of connections effectively increases the enthalpy, ΔH, between particles and, therefore, raises the melting temperature, T_m [16].

For short DNA (12–14 base pairs), melting and hybridization can be described by a two-state model as an equilibrium between single- and double-stranded DNA [22],

$$S + S \rightleftharpoons D .$$
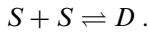
The melting curve is a slowly varying function of temperature and can be described by the van't Hoff relationship [21]. While short, free DNA does not exhibit a phase transition, DNA bound to nanoparticles aggregate to form networks that have a definite phase transition, and the melting curves cannot be described with the van't Hoff relationship.

The DNA-linked gold nanoparticle assemblies have several unusual features, including a sharp melting transition compared to that of corresponding free DNA, and the melting temperature, T_m, dependence on colloid size [18,24,25]. Recently, simulations based on the bond percolation model [16,26] agree qualitatively with the experimental optical spectra of DNA-capped gold colloids at the melting transition. It has been suggested that at percolation, $[1 - p(T_c)]^{N_s/z} = 1 - p_c$, where N_s, z, p_c, T_c are the number of single-stranded DNA on each gold particle, number of nearest neighbors per gold particle, bond percolation threshold, and melting temperature, respectively [16]. The fraction of single-stranded DNA that form links is $p(T)$ and is temperature dependent. The melting transition occurs when the fraction of links falls below the percolation threshold. The calculated optical properties are found to change dramatically when this threshold is passed. Moreover, the size dependence of melting temperature can be explained in terms of the effect on link fraction. The number of DNA on each particle, N_s, increases with increasing particle size, D, with the relation $N_s \propto D^2$. The simulation confirmed the melting temperature dependence on particle size. Therefore, the percolation model can qualitatively explain the experimental findings.

The experimental results used for comparison, however, have two kinds of particles, denoted as an AB system since each particle is either covered with $DNA1$ (denoted as particle A) or $DNA2$ (denoted as particle B), but not both, and particle A can only be linked to particle B. Fig. 4a illustrates such a binary system. In most simulations, the system is composed of only one kind of particle, and each particle can be linked with any other particle. To this end, we studied an AA system, where each particle is covered with both $DNA1$ and $DNA2$. This results in only one type of nanoparticle, and each particle can be linked with any other particle in the system, as shown in Fig. 4b.

Melting curves for AA and AB systems are shown in Fig. 5. We noted that the width of the melting transition in the AA system is much narrower than that of the AB system. The scaling of melting temperature with particle size is also different for AA and AB systems. Unlike the AB system, there are $DNA1$ and $DNA2$ on the same particle in the AA system. Since $DNA1$ only connects with $DNA2$, the connections in the AA system is different from that in the AB. More experimental data on the
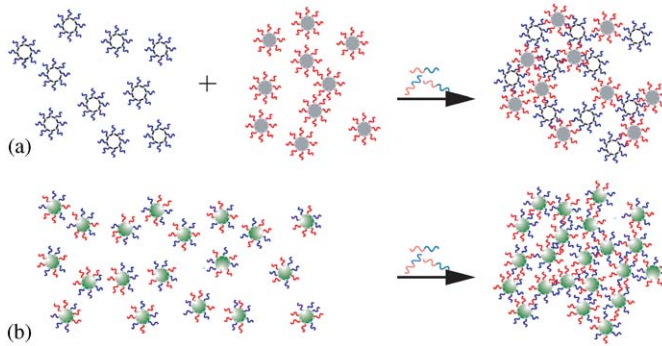
Fig. 4. Compositions of the *AA* versus *AB* systems. (a) In the *AB* system, each particle is covered with with either *DNA*1 or *DNA*2 to create probes *A* and *B*, respectively. *DNA*1 and *DNA*2 are not complementary, and the linker DNA is complementary to *DNA*1 and *DNA*2. As a result, probe *A* binds exclusively with probe *B* upon the introduction of a target DNA sequence. (b) In the *AA* system, each particle is covered with both *DNA*1 and *DNA*2 at a 1:1 ratio, resulting in only one type of probe (*A*). Hence each particle can bind with any other particle in the solution.
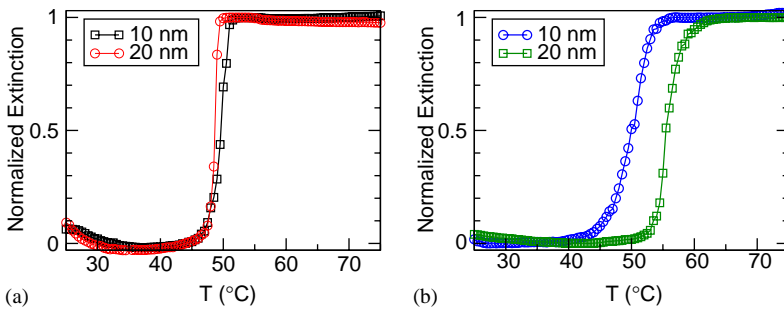

Fig. 5. Melting curves for (a) *AA* and (b) *AB* nanoparticle systems monitored at 260 nm. In the *AB* (binary particle) system, particle *A* can only bind with particle *B* and vice versa, whereas in the *AA* system there is only one type of particle. The melting transition width is different and the melting temperature scales differently for the *AA* and *AB* systems.

melting curves of *AA* systems of different particle sizes are necessary to elucidate how the trend in melting temperature changes from the *AB* to the *AA* systems.

In general, the percolation model is a crude representation of any gelation process [27]. In practice, the DNA-capped gold colloids are mixed with a solvent, and this can be considered as "dilution effect," i.e., gelation in dilute solution. A gelation process in the presence of solvent always brings a trend toward phase separation of the gelating species, and the phase diagram is illustrated in Fig. 6. However, the critical exponents observed in our system may be of the percolation type, as predicted by de Gennes [27], and supported by simulations [16].
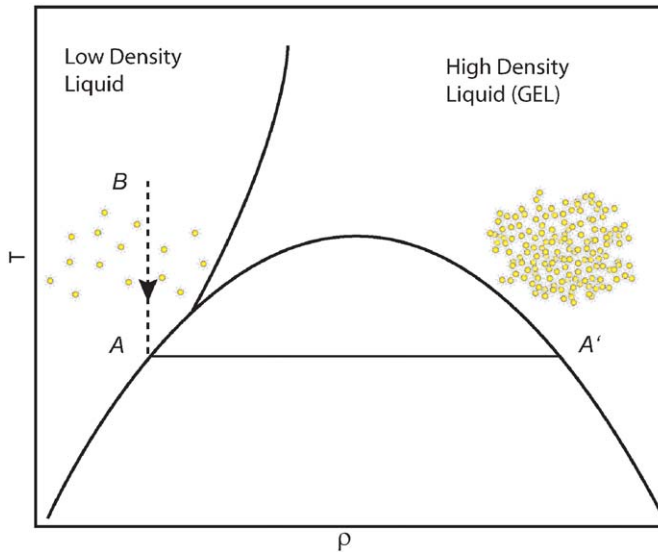
Fig. 6. Proposed phase diagram of a DNA-linked colloidal gold system. The gelation in the presence of solvent results in phase separation below the transition temperature. The experiment follows the dashed line to the liquid/gel phase separation.

As Lukatsky and Frenkel [3] recently proposed, the equilibrium phase behavior of DNA-linked colloidal assemblies is dominated by the temperature-dependent binding free energy of a double-stranded DNA connecting a pair of gold colloidal particles. Depending on the strength of the interaction, the system can be in a homogeneous state, or separate into two coexisting phases. Their calculation shows that there is a liquid–liquid phase separation in DNA-linked gold nanoparticle assemblies. The origin of the sharp phase transition is the entropic cooperativity of DNA-nanoparticle network. Upon cooling, the system undergoes liquid–liquid phase separation. The dense liquid phase is strongly cross-linked and behaves as a solid gel.

For our systems, we did observe phase separation, as predicted by de Gennes [27]. TEM images give direct evidence of the formation of the gel phase, and support the expectation of phase transition and separation. As shown in Fig. 2, upon adding linker DNA, gold colloids form gel-like porous and amorphous aggregates. Phase separation occurs and eventually the dense aggregates precipitate out of the solution, and the solution eventually becomes clear.

3. Summary

We have presented direct evidence of a liquid–gel phase transition of the DNA-linked gold colloidal assemblies. Compared to free DNA, a sharp melting transition

is observed for this system. The formation of DNA-linked gold colloids and the sharpness of the melting transition resemble the phase behavior of gelation in dilute solution phenomena. We have shown that the scaling property of the binary system *AB*, where two types of particles exists, is different from that of *AA*, where all the particles are of the same type. The results shown here indicate that the DNA-linked gold nanoparticles represent a new class of complex fluids.

References

[1] D. Frenkel, Soft condensed matter, Physica A 313 (2002) 1–31.

[2] K. t Leung, B. Schmittmann, R.K.P. Zia, Phase transitions in a driven lattice gas with repulsive interactions, Phys. Rev. Lett. 62 (1989) 1772–1775.

[3] D.B. Lukatsky, D. Frenkel, Phase behavior and selectivity of DNA-linked nanoparticle assemblies, Phys. Rev. Lett. 92 (2004) 068302.

[4] A.V. Tkachenko, Morphological diversity of DNA-colloidal self-assembly, Phys. Rev. Lett. 89 (2002) 148303-1–148303-4.

[5] D.K. Lubensky, D.R. Nelson, Pulling pinned polymers and unzipping DNA, Phys. Rev. Lett. 85 (2000) 1572–1575.

[6] Y. Zeng, A. Montrichok, G. Zocchi, Length and statistical weight of bubbles in DNA melting, Phys. Rev. Lett. 91 (2003) 148101-1–148101-4.

[7] G. Zocchi, A. Omerzu, T. Kurabova, J. Rudnick, G. Grüner, Duplex-single strand denaturing transition in DNA oligomers, arXiv:cond-mat/0304567 v1.

[8] R.M. Wartell, A.S. Benight, Thermal denaturation of DNA molecules: a comparison of theory with experiment, Phys. Rep. 126 (1985) 67–107.

[9] D. Cule, T. Hwa, Denaturation of heterogeneous DNA, Phys. Rev. Lett. 79 (1997) 2375–2378.

[10] M.E. Fisher, Effect of excluded volume on phase transitions in biopolymers, J. Chem. Phys. 45 (1966) 1469–1473.

[11] M.S. Causo, B. Coluzzi, P. Grassberger, Simple model for the DNA denaturation transition, Phys. Rev. E 62 (2000) 3958–3973.

[12] C.A. Gelfand, G.E. Plum, S. Mielewczyk, D.P. Remeta, K.J. Breslauer, A quantitative method for evaluating their stabilities of nucleic acids, Proc. Natl. Acad. Sci. USA 96 (1999) 6113–6118.

[13] F. Naef, D.A. Lim, N. Patil, M. Magnasco, DNA hybridization to mismatched templates: a chip study, Phys. Rev. E 65 (2002) 040902-1–040902-4.

[14] C.A. Mirkin, R.L. Letsinger, R.C. Mucic, J.J. Storhoff, A DNA-based method for rationally assembling nanoparticles into macroscopic materials, Nature 382 (1996) 607–609.

[15] A.P. Alivisatos, K.P. Johnsson, X. Peng, T.E. Wilson, C.J. Loweth, M.P. Bruchez Jr., P.G. Schultz, Organization of nanocrystal molecules using DNA, Nature 382 (1996) 609–611.

[16] S.Y. Park, D. Stroud, Theory of melting and the optical properties of gold/DNA nanocomposites, Phys. Rev. B 67 (2003) 212202.

[17] V.J. Anderson, H.N.W. Lekkerkerker, Insights into phase transition kinetics from colloid science, Nature 416 (2002) 811–815.

[18] C.-H. Kiang, Phase transition of DNA-linked gold nanoparticles, Physica A 321 (2003) 164–169.

[19] E.R. Weeks, J.C. Croker, A.C. Levitt, A. Schofield, D.A. Weitz, Three-dimensional direct imaging of structural relaxation near the colloidal glass transition, Science 287 (2000) 627–631.

[20] C.-H. Kiang, Single particle study of protein assembly, Phys. Rev. E 64 (2001) 041911-1–041911-3.

[21] C.R. Cantor, P.R. Schimmel (Eds.), Biophysical Chemistry, Part II: Techniques for the Study of Biological Structure and Function, W.H. Freeman and Company, New York, 1980.

[22] V.A. Bloomfield, D.M. Crothers, I. Tinoco Jr., Nucleic Acids, University Science Books, California, 2000.

[23] L.M. Demers, C.A. Mirkin, R.C. Mucic, R.A. Reynolds III, R.L. Letsinger, R. Elghanian, G. Viswanadham, A fluorescence-based method for determining the surface coverage and hybridization

efficiency of thiol-capped oligonucleotides bound to gold thin films and nanoparticles, Anal. Chem. 72 (2000) 5535–5541.

[24] Y. Sun, N.C. Harris, C.-H. Kiang, Melting transition of directly linked gold nanoparticle DNA assembly, Physica A 350 (2005) 89.

[25] N.C. Harris, C.-H. Kiang, Disorder in DNA-linked gold nanoparticle assemblies, submitted for publication.

[26] S.Y. Park, D. Stroud, Structure formation, melting, and optical properties of gold/DNA nanocomposites: effects of relaxation time, Phys. Rev. B 68 (2003) 224201.

[27] P.-G. de Gennes, Scaling Concepts in Polymer Physics, Cornell University Press, Ithaca, 1979, pp. 148–152.